

RESEARCH ARTICLE

# A revised understanding of *Tribolium* morphogenesis further reconciles short and long germ development

Matthew A. Benton\*

Department of Zoology, University of Cologne, Cologne, Germany

\* [matthewabenton@gmail.com](mailto:matthewabenton@gmail.com)



**OPEN ACCESS**

**Citation:** Benton MA (2018) A revised understanding of *Tribolium* morphogenesis further reconciles short and long germ development. PLoS Biol 16(7): e2005093. <https://doi.org/10.1371/journal.pbio.2005093>

**Academic Editor:** Claude Desplan, New York University, United States of America

**Received:** December 11, 2017

**Accepted:** June 15, 2018

**Published:** July 3, 2018

**Copyright:** © 2018 Matthew A. Benton. This is an open access article distributed under the terms of the [Creative Commons Attribution License](https://creativecommons.org/licenses/by/4.0/), which permits unrestricted use, distribution, and reproduction in any medium, provided the original author and source are credited.

**Data Availability Statement:** All relevant data are within the paper and the Supporting Information files. Additional data from the differential cell labeling timelapse experiments are available from the 'figshare' database ([https://figshare.com/authors/Matthew\\_Benton/4693354](https://figshare.com/authors/Matthew_Benton/4693354)).

**Funding:** Alexander von Humboldt Foundation <https://www.humboldt-foundation.de/web/home.html>. Postdoctoral fellowship. The funder had no role in study design, data collection and analysis, decision to publish, or preparation of the manuscript.

## Abstract

In *Drosophila melanogaster*, the germband forms directly on the egg surface and solely consists of embryonic tissue. In contrast, most insect embryos undergo a complicated set of tissue rearrangements to generate a condensed, multilayered germband. The ventral side of the germband is embryonic, while the dorsal side is thought to be an extraembryonic tissue called the amnion. While this tissue organisation has been accepted for decades and has been widely reported in insects, its accuracy has not been directly tested in any species. Using live cell tracking and differential cell labelling in the short germ beetle *Tribolium castaneum*, I show that most of the cells previously thought to be amnion actually give rise to large parts of the embryo. This process occurs via the dorsal-to-ventral flow of cells and contributes to germband extension (GBE). In addition, I show that true 'amnion' cells in *Tribolium* originate from a small region of the blastoderm. Together, my findings show that development in the short germ embryos of *Tribolium* and the long germ embryos of *Drosophila* is more similar than previously proposed. Dorsal-to-ventral cell flow also occurs in *Drosophila* during GBE, and I argue that the flow is driven by a conserved set of underlying morphogenetic events in both species. Furthermore, the revised *Tribolium* fate map that I present is far more similar to that of *Drosophila* than the classic *Tribolium* fate map. Lastly, my findings show that there is no qualitative difference between the tissue structure of the cellularised blastoderm and the short/intermediate germ germband. As such, the same tissue patterning mechanisms could function continuously throughout the cellularised blastoderm and germband stages, and easily shift between them over evolutionary time.

## Author summary

In many animals, certain groups of cells in the embryo do not directly contribute to the formation of adult structures. Instead, these so-called 'extraembryonic tissues' that support and facilitate development are discarded and degenerate prior to birth/hatching. Embryos of most insect species are thought to have two types of extraembryonic tissues: the serosa, which encapsulates the entire embryo and yolk, and the amnion, which covers only half of the embryo. Descriptions of the amnion have been widely reported for over a

**Competing interests:** The authors have declared that no competing interests exist.

**Abbreviations:** AP, anterior-posterior; BMP, *Bone Morphogenetic Protein*; DV, dorsoventral; EL, egg length; GBE, germband extension; NLS-tdEos, *nuclear localisation signal-tandem Eos*; SAZ, *segment addition zone*; Tc-srp, *Tribolium* ortholog of the GATA factor *serpent*; YFP, *yellow fluorescent protein*.

century, but detailed studies of this tissue are lacking. Here I used imaging and tracking techniques to investigate amnion development in the beetle *Tribolium castaneum* embryo. In contrast to our current understanding, I show that most cells previously thought to be part of the amnion constitute large regions of the embryo. In addition, I show that these cells ‘flow’ as a whole tissue and contribute to the elongation of the embryo, and only a relatively small number of cells form the actual amnion. This resemblance to the well-studied germband in the fruit fly, *Drosophila melanogaster*, shows that despite exhibiting substantial differences in the overall structure, embryos of beetles and flies share a conserved set of morphogenetic processes.

## Introduction

Insects are the most speciose phylum of animals and display remarkable diversity in adult morphology [1]. Insect embryo development is also very diverse, particularly in the stages leading to the formation of the elongated, segmented embryo (called the germband) [2]. The molecular and morphogenetic basis of this process is best understood in the fly *Drosophila melanogaster*. In this species, a predominantly hierarchical chain of patterning events specifies nearly all segments more or less simultaneously at the syncytial blastoderm stage [3]. Cellularisation takes place near the end of this process, after which point morphogenetic events such as germband extension (GBE) occur (see Fig 1 for schematic summary). The *Drosophila* mode of development is termed long germ development and is fairly representative of most true flies [4]. In contrast, the vast majority of insects undergo short or intermediate germ development, meaning that only a handful of segments are specified at the blastoderm stage and the remaining segments are specified sequentially as the germband elongates [5].

Short germ development has been best studied in the beetle *Tribolium castaneum*, and recent research has shown that development in this species is more similar to *Drosophila* than previously thought. In *Drosophila*, GBE is predominantly driven by the mediolateral intercalation of ectodermal cells (i.e., convergent extension), although cell deformation along the anterior-posterior (AP) axis and cell divisions are also involved [6–11]. In contrast to this, *Tribolium* germband elongation was previously thought to be driven by the so-called ‘growth zone’ at the posterior of the germband [12]. Now, however, it is clear that *Tribolium* germband elongation is also predominantly driven by mediolateral cell intercalation (see Fig 1 for schematic summary of *Tribolium* development) [13–15]. Furthermore, in both *Tribolium* and *Drosophila*, this intercalation requires the striped expression of a specific group of Toll genes (so-called Long Toll/Loto class genes) [16,17].

It is highly likely that germband elongation mediated by cell intercalation is homologous in these two species, and probably in other arthropods, as well [17]. As such, I will hereafter refer to *Tribolium* ‘germband elongation’ as ‘germband extension’/GBE, unifying the *Drosophila*/*Tribolium* terminology. In addition, as there is no evidence for a qualitatively different ‘growth zone’ in *Tribolium* (i.e., a specialised zone of volumetric growth), I will refer to the posterior unsegmented region as the segment addition zone (SAZ) [19–21].

Despite the similarities described above, there are substantial differences in the embryonic fate maps of these two species (Fig 1). In *Drosophila*, almost the entire blastoderm is fated as embryonic tissue, and only a small dorsal region is fated as extraembryonic tissue (termed the amnioserosa) [18]. In contrast, in *Tribolium*, roughly the anterior third of the blastoderm gives rise to an extraembryonic tissue called the serosa [22]. Of the remaining blastoderm, a large dorsal region is thought to give rise to a second extraembryonic tissue called the amnion, with

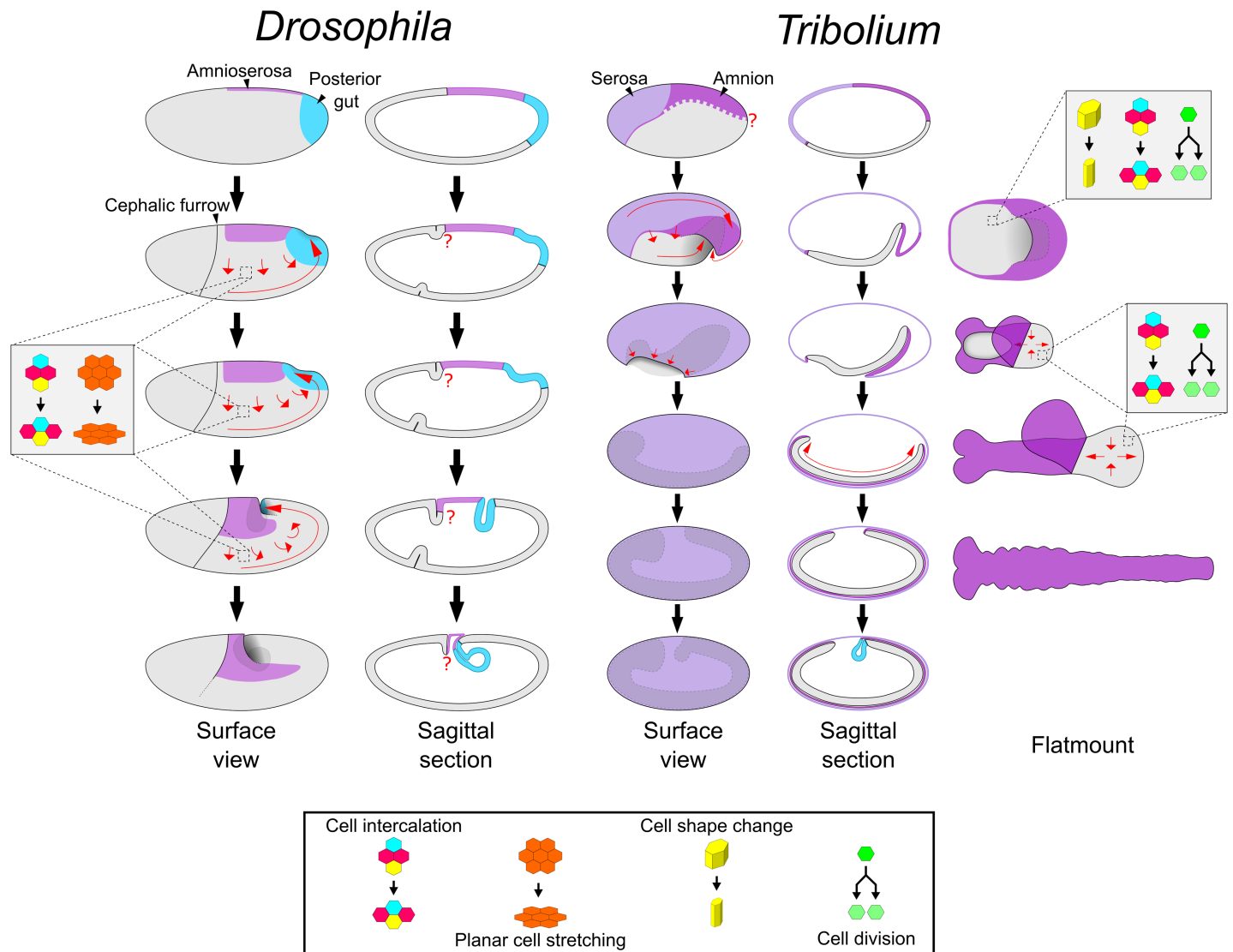


**Fig 1. Schematics of development in *Drosophila* and *Tribolium*.** The two left columns show schematics of *Drosophila* embryos from the uniform blastoderm stage to the extended germband stage. The right three columns show schematics of *Tribolium* embryos at comparable developmental stages. The schematics in the rightmost column depict dissected, flat-mounted embryos. Red arrows display cell/tissue movement. The question marks highlight two regions (the *Drosophila* embryo/amnioserosa border in the cephalic furrow region, and the dorsoventral position of the *Tribolium* embryo/amnion border) where the tissue boundaries are unknown/undescribed. Several features have been omitted, including the yolk, mesoderm gastrulation, anterior gut formation, and appendage formation. The *Drosophila* fate map is based on data from [18] and the references therein. Refer to text for additional details.

<https://doi.org/10.1371/journal.pbio.2005093.g001>

only the remaining ventral tissue giving rise to the embryo itself [23–25]. Like the amnioserosa, the serosa and the amnion are proposed to support the embryo during development but are thought to degenerate prior to hatching and not contribute to any larval or adult structures [19,26,27].

*Drosophila* and *Tribolium* also exhibit dramatic differences in the morphogenetic events occurring during early development (Fig 1). When GBE occurs in *Drosophila*, the germband stays at the surface of the egg and the amnioserosa largely remains in place. In *Tribolium*, on the other hand, GBE begins with a process called embryo condensation, during which the embryonic ectoderm and presumptive amnion (together termed the ‘germ rudiment’) form the germband (see Fig 1; for a detailed description, see [14,28]). Several concurrent morphogenetic

events underlie embryo condensation. The embryonic ectoderm condenses towards the ventral side of the egg via both mediolateral cell intercalation and a cuboidal-to-columnar cell shape transition. Simultaneously, epithelial folding and tissue involution occurs, causing the presumptive amnion to fold over the embryonic ectoderm. During these movements, the serosa cells undergo a cuboidal-to-squamous transition to spread over the entire egg surface. The final stage of embryo condensation coincides with closure of the serosa (serosa window stage), which appears to involve a supracellular actomyosin cable [14].

The differences in fate map and tissue folding described above show that both fate map shifts and reductions in early morphogenetic events have contributed to the evolution of the long germ mode of development found in *Drosophila*. However, it is important to note that *Drosophila*, regarding the extraembryonic tissues, represents an extreme case of reductive evolution, which is characteristic only for higher cyclorrhaphan flies [29]. More basally branching flies form both an amnion and a serosa, while still exhibiting the long germ mode of development (for a review, see [26]). For example, in the scuttle fly *Megaselia abdita*, both an amnion and serosa form, but while the serosa spreads over the egg surface as in *Tribolium*, the amnion remains at the dorsal side of the embryo, similar to the *Drosophila* amnioserosa [30–33]. Such intermediate topologies help to explain the evolution of the situation in *Drosophila*, in which all extraembryonic cells remain at the dorsal side.

Understanding how these differences evolved is integral to understanding the short-to-long germ transition, but in order to study how this occurred, we first need to understand how these tissues develop in each species. The form and function of the *Tribolium* serosa has been analysed in several studies [22,34,35]. The amnion, on the other hand, has proven harder to analyse, and the precise embryo/amnion boundary at the blastoderm stage is unknown. However, a defined boundary between embryo and amnion has been proposed to exist from when the germband forms (Fig 1) [23]. Cells in the ventral half of the germband (ventral with respect to the germband dorsoventral [DV] polarity, but dorsal with respect to the egg) are thought to give rise to all embryonic structures, while cells in the dorsal half of the germband (dorsal with respect to the germband DV polarity, but ventral with respect to the egg) are thought to form the amnion [25,36,37]. This germband structure has been described in many insects over the past century and is proposed to represent the core conserved structure of short/intermediate germ embryos (reviewed in [2,38,39]). However, the proposed boundary between cells fated to become embryo and those fated to become amnion has not been directly tested.

Here, I investigate the development of the presumptive amnion in *Tribolium* using a combination of fluorescent live imaging and fate mapping techniques. To my great surprise, I find that the majority of the cells previously described as ‘amnion’ actually form large parts of the embryo proper. Using fate-mapping experiments, I show that true ‘amnion’ cells originate from a very small domain of the blastoderm, just as the *Drosophila* amnioserosa cells do. I also show that the movement of cells from the ‘amnion’ side of the germband to the ‘embryo’ side of the germband occurs via the large-scale flow of the ectodermal epithelium. Lastly, I describe the underlying causes of this flow, and show how this tissue movement is likely homologous to the dorsal-to-ventral tissue flow that occurs during *Drosophila* GBE.

## Results

### Live cell tracking reveals movement of ‘amnion’ cells into the embryo

To examine the development of the *Tribolium* presumptive amnion in detail, I carried out high resolution live imaging of embryos transiently labelled [14] with a fluorescent histone marker (H2B-venus) to label nuclei. My goal was to track presumptive amnion cells from the blastoderm stage onwards. However, it was not possible to accurately track the majority of

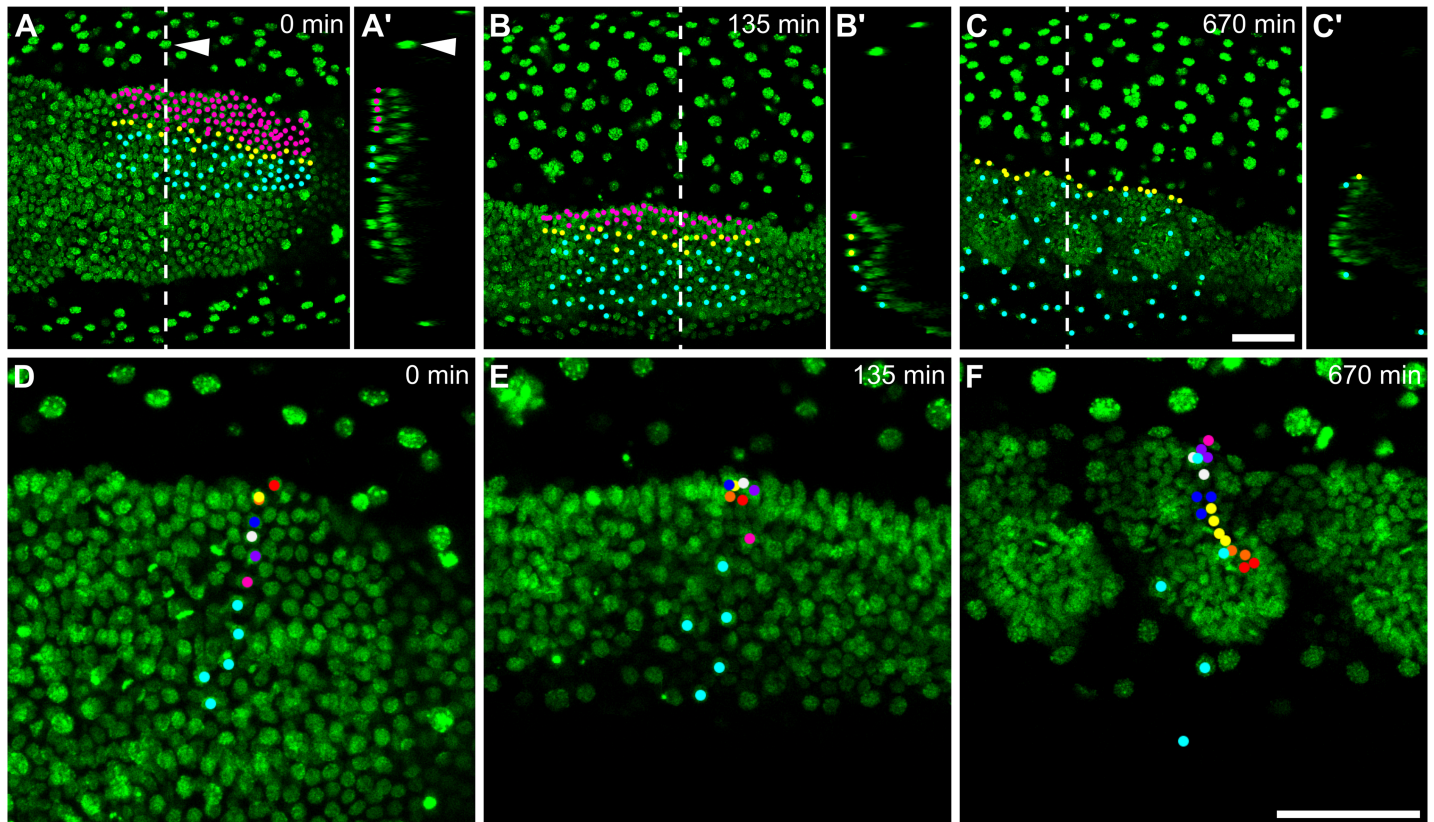


**Fig 2. Live cell tracking reveals contribution of ‘amnion’ cells to embryonic tissue.** (A–F) Time series from fluorescent live imaging of a *Tribolium* embryo expressing H2B-venus. The serosa nuclei located above the germband have been manually removed from these frames (by deleting them from individual z-stack slices) but left in the surrounding territory (arrowhead in [A+A’]). (A’–C’) show optical transverse sections of the respective frame at the position shown by the dashed line (the surface of the egg is to the left). In (A–C), all nuclei that lie in a region of the ‘amnion territory’ in (A) have been tracked and differentially labelled depending on whether they become part of the embryo (magenta; labels disappear when nuclei join the germband), become located at the edge of the germband (yellow), or remain in the ‘amnion territory’ (cyan). In (D–F), a line of nuclei that lie in the ‘amnion territory’ in (D) have been tracked and differentially labelled depending on whether they become part of the embryo (coloured points; daughter cells are labelled in same colour as parent) or remain in the ‘amnion territory’ (cyan; no division takes place). Note that in panel (D), the orange spot is mostly hidden below the yellow spot because the nuclei in that region are partially overlapping when viewed as projections. The first frame of the timelapse was defined as time point 0. In (A–F), embryos are oriented based on the AP/DV polarity of the egg, with anterior to the left and dorsal to the top. (A–C) are maximum intensity projections of one egg hemisphere. (D–F) are average intensity projections of 46 microns to specifically show the germband. Scale bars are 50  $\mu$ m. AP, anterior-posterior; DV, dorsoventral.

<https://doi.org/10.1371/journal.pbio.2005093.g002>

cells throughout embryo condensation and GBE because of the extensive morphogenetic rearrangements that take place during this process. Instead, I focused on the stage immediately following condensation, when the germband has formed, and analysed the embryonic region where the presumptive amnion is closest to the surface of the egg. Specifically, I tracked over 200 presumptive amnion cells from the central region of the germband from the closure of the serosa window until after the formation of the thoracic segments (over 11 hours of development; Fig 2 and S2 Movie). As previously described [14], the germband and yolk exhibit pulsatile movements during this period, as well as rotating within the serosa (S1 Movie).

The presumptive amnion initially consists of many tightly packed cells, which become increasingly spread out during GBE (S2 Movie, Fig 2A–2C). However, rather than remaining restricted to the ‘amnion territory’, many of the tracked cells moved around the edge of the germband into the ‘embryo territory’. Differential labelling of tracked cells clearly showed that these cells that moved around the germband edge became part of the embryo proper (S2 Movie and Fig 2A–2C). The cells that joined the ‘embryo territory’ became tightly packed, continued

to divide, and formed embryonic structures (S3 Movie and Fig 2D–2F). In contrast, cells that remained in the ‘amnion territory’ became squamous and stopped dividing. The nuclei of these latter cells became enlarged (S3 Movie and Fig 2D–2F), suggesting that they underwent endoreplication to become polyploid, as seen in the *Tribolium* serosa and in the *Drosophila* amnioserosa [18,24]. In addition, several germband nuclei underwent apoptosis (S3 Movie), as has been described in fixed embryos [40]. These results show that many of the cells previously thought to constitute extraembryonic amnion give rise to embryonic structures.

Because the epithelium formerly termed ‘amnion’ is made up cells that will variously form amnion, dorsal ectoderm, and dorsolateral ectoderm, it is not accurate for the entire tissue to be called ‘amnion’. Therefore, I will refer to this part of the germband as the ‘dorsal epithelium’, based on the tissue’s location at the dorsal side of the germband (with respect to the DV polarity of the germband rather than the egg). This term ‘dorsal epithelium’ is simply a spatial designation and comes with no implicit assumptions about the identity of the tissue nor the final fate of the tissue. It is also important to keep in mind that the dorsal epithelium is continuous with the ventral epithelium.

### Differential cell labelling confirms widespread dorsal-to-ventral cell movement

My next question was whether the movement of cells from the dorsal epithelium to the ventral epithelium occurs throughout the AP axis or is just limited to the thoracic region. The extensive movements of the germband made it difficult to track individual cells accurately at the anterior and posterior poles. To overcome this problem, I combined differential cell labelling with long-term fluorescent live imaging to follow small groups of nuclei throughout development. Specifically, I microinjected mRNA encoding a nuclear-localised photoconvertible fluorescent protein (nuclear localisation signal-tandem Eos [NLS-tdEos]) into pre-blastoderm embryos to uniformly label all nuclei, then photoconverted a small patch of nuclei at different positions along the AP axis at the final uniform blastoderm stage. I then performed long-term confocal live imaging of both the unconverted and photoconverted forms of the fluorescent protein throughout the period of GBE (or longer). Unlike that of *Drosophila*, the *Tribolium* eggshell does not show any DV polarity, and I was therefore unable to specifically target particular locations along the DV axis. Instead, I opted for a brute-force approach and performed the photoconversion experiment at unknown DV positions for 50–150 embryos at each of the following AP positions: 75% egg length (EL) from the posterior pole, 50% EL, 25% EL, and close to the posterior pole. I then used the resulting live imaging data to determine the approximate DV position of the photoconverted cells. Using a new live imaging setup (see [Materials and methods](#)), I obtained the same range of hatching rates as I typically obtain for other microinjection experiments (approximately 80% [14]), even after continuous confocal live imaging for almost the entirety of *Tribolium* embryonic development (3.5 days; S4 Movie). Both unconverted and photoconverted protein persisted throughout GBE and retraction, although fluorescent signal faded over time. I have included various examples from this data set in S1–S3 Figs. In addition, I have made the raw confocal data for a large number of timelapses available online (>300 embryos, >700 GB of data [41]) for the benefit of the community. These data will likely prove valuable for a wide range of research projects.

When I examined clones initially located in the dorsal epithelium, I found that movement of cells from the dorsal epithelium to the ventral epithelium occurred throughout the posterior of the embryo during GBE (Fig 3A–3F, S5 Movie). I also observed the same movements at the anterior of the germband (Fig 3G–3J), although I have focused my analysis on the middle and posterior parts of the embryo. Together with the cell tracking data, these results show that

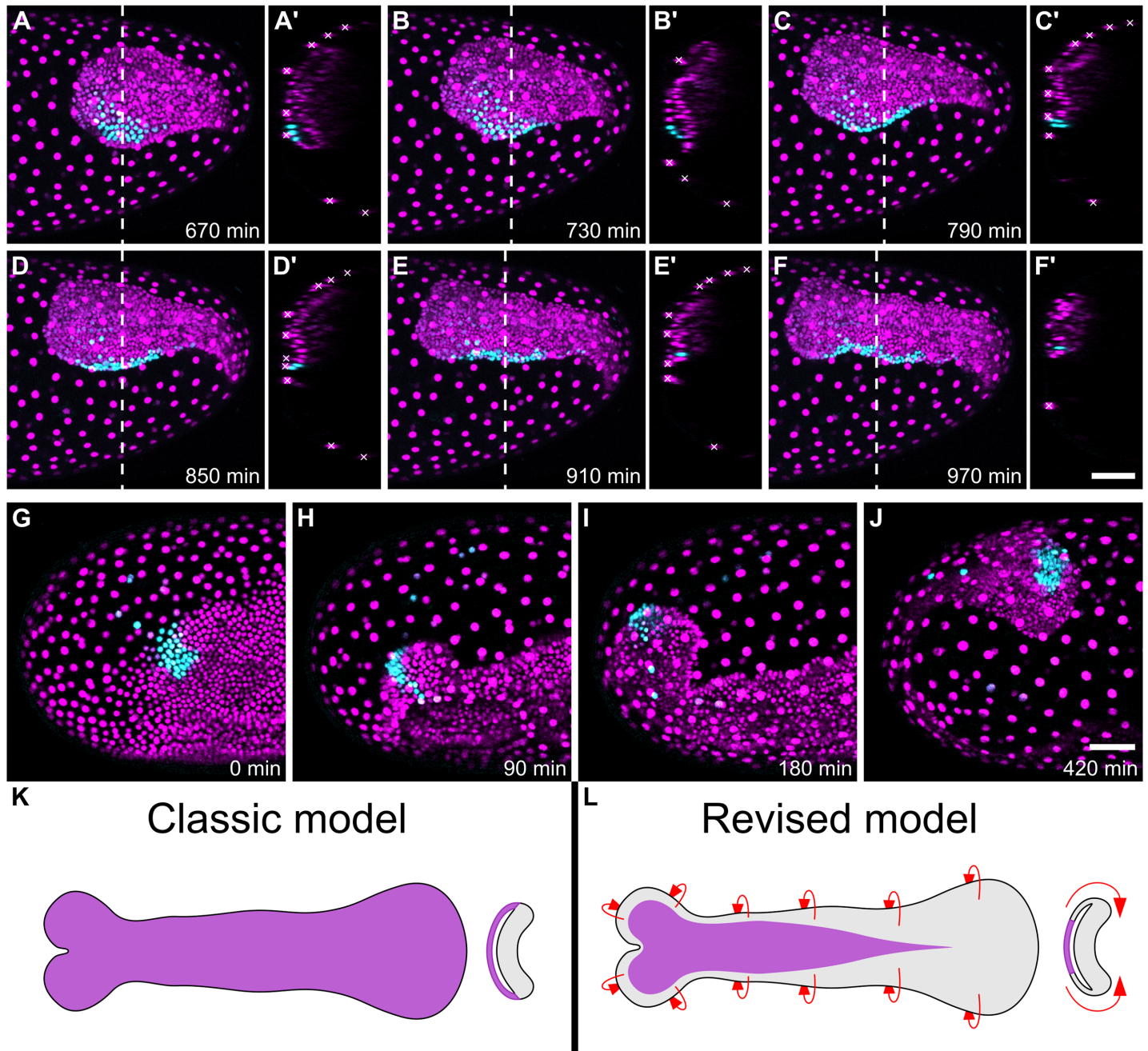


**Fig 3. Differential cell labelling reveals widespread movement of cells from the dorsal epithelium to the ventral epithelium.** (A-J) Time series from fluorescent live imaging of two *Tribolium* embryos expressing NLS-tdEos showing unconverted protein (magenta) and photoconverted protein (cyan). In (A-F'), a patch of nuclei at the posterior-dorsal region of the blastoderm was photoconverted. Panels (A-F) show the posterior region of the germband during late GBE, and panels (A'-F') show optical transverse sections made at the position of the dashed line at each time point (roughly following the same nuclei). Serosa nuclei are marked by white crosses in the transverse sections. In (G-J), a patch of nuclei at the anterior-lateral region of the blastoderm was photoconverted. Panels (G-J) show the anterior of the germband during condensation and GBE. In both embryos, all converted nuclei are initially located in the dorsal epithelium, but most move into the ventral epithelium during GBE. (K-L) Schematics showing the classic and revised models of the *Tribolium* germband (presumptive amnion is shown in purple, presumptive embryo is shown in grey, and red arrows show the newly discovered tissue flow). The first frame of the timelapses was defined as time point 0. In (A-J), embryos are oriented based on the AP/DV polarity of the egg, with anterior to the left and dorsal to the top. In (A'-F'), the surface of the egg is oriented to the left. In (K-L), schematics show flat-mounted germbands with the focus on the dorsal epithelium, the anterior to the left, and the orthogonal sections are oriented with the dorsal half of the germband to the left. (A-J) are maximum intensity projections of one egg hemisphere. Scale bars are 50  $\mu$ m. AP, anterior-posterior; DV, dorsoventral; GBE, germband extension; NLS-tdEos, nuclear localisation signal-tandem Eos.

<https://doi.org/10.1371/journal.pbio.2005093.g003>

most of what was previously thought to be ‘amnion’ is in fact embryonic tissue, and that cells move from the dorsal epithelium to the ventral epithelium throughout the germband (summarised in [Fig 3K and 3L](#))).

### Mediolateral cell intercalation occurs throughout GBE

During my live imaging, ectodermal cell clones became elongated along the AP axis over time, as previously reported in a *Tribolium* study that used a non-live imaging cell clone method [15]. However, this study found that ‘labelled ectodermal cells. . .rarely mix with unlabelled cells’, even as clones became greatly elongated [15]. In contrast, I frequently observed nonconverted nuclei in the midst of labelled nuclei ([Fig 3, S1–S3 Figs](#)).

To test whether the pattern I observed was caused by mediolateral cell intercalation, I tracked the nuclei of abutting rows of ectodermal cells in the SAZ during formation of the abdominal segments (50 cells in total, tracked for 3.5 hours; [Fig 4 and S6 Movie](#)). This analysis clearly showed that, as during embryo condensation [14], cells intercalated between their dorsal and ventral neighbours. Together with the photoconversion data set, these results show that extensive mediolateral cell intercalation takes place throughout GBE to drive the convergent extension of the ectoderm.

### *Tribolium serpent* may mark true ‘amnion’

As described earlier, cells that remained in the dorsal epithelium became squamous, and this cell shape change occurred progressively along the AP axis ([Fig 5A](#)). This change in cell shape may be a sign of maturation of true ‘amnion’. While characterising cell fate markers, I found that the *Tribolium* ortholog of the GATA factor *serpent* (*Tc-srp*) exhibited spatial and temporal expression dynamics that were very similar to those of the potential ‘amnion’ (i.e., progressive flattening of cells, [Fig 5B, S4 Fig](#)).

At the end of GBE, all but the most posterior cells of the dorsal epithelium were squamous and *Tc-srp* seemed to be expressed in dorsal epithelium cells along nearly the full length of the germband ([S4 Fig\(I<sub>2</sub>\)](#)). However, this latter finding was difficult to confirm, as most of the dorsal epithelium is lost during embryo fixation at this embryonic stage (presumably due to the fragility of the tissue). I also found *Tc-srp* to be expressed in several other domains, including in the presumptive endoderm ([S4 Fig](#)).

In *Drosophila*, *serpent* is also expressed in extraembryonic tissue (the amnioserosa) [42–45], and, therefore, *Tc-srp* may mark ‘true’ extraembryonic amnion. However, future work is required to confirm whether this putative amnion degenerates prior to hatching (as is required to be defined as extraembryonic). For simplicity, I will refer to this tissue as ‘amnion’ for the remainder of this text.

### A revised *Tribolium* amnion fate map

To determine which blastoderm cells give rise to the amnion, I analysed 85 embryos in which the dorsal and dorsolateral blastoderm cells were labelled by NLStdEos photoconversion as described above. As I was unable to determine the precise DV position of the photoconverted cells at the blastoderm stage, I (1) examined embryos at the extended germband stage (when the mature amnion had formed), (2) determined the embryos in which photoconverted nuclei spanned the full DV width of the amnion (but were not observed in the embryonic tissue), and (3) checked the initial size of the photoconverted patch of nuclei (for a schematic of this approach, see [S5 Fig](#)).

I found that amnion cells arose from a very small domain of dorsalmost cells (that tapers from its anterior to posterior extent) and from a narrow strip of cells between the presumptive

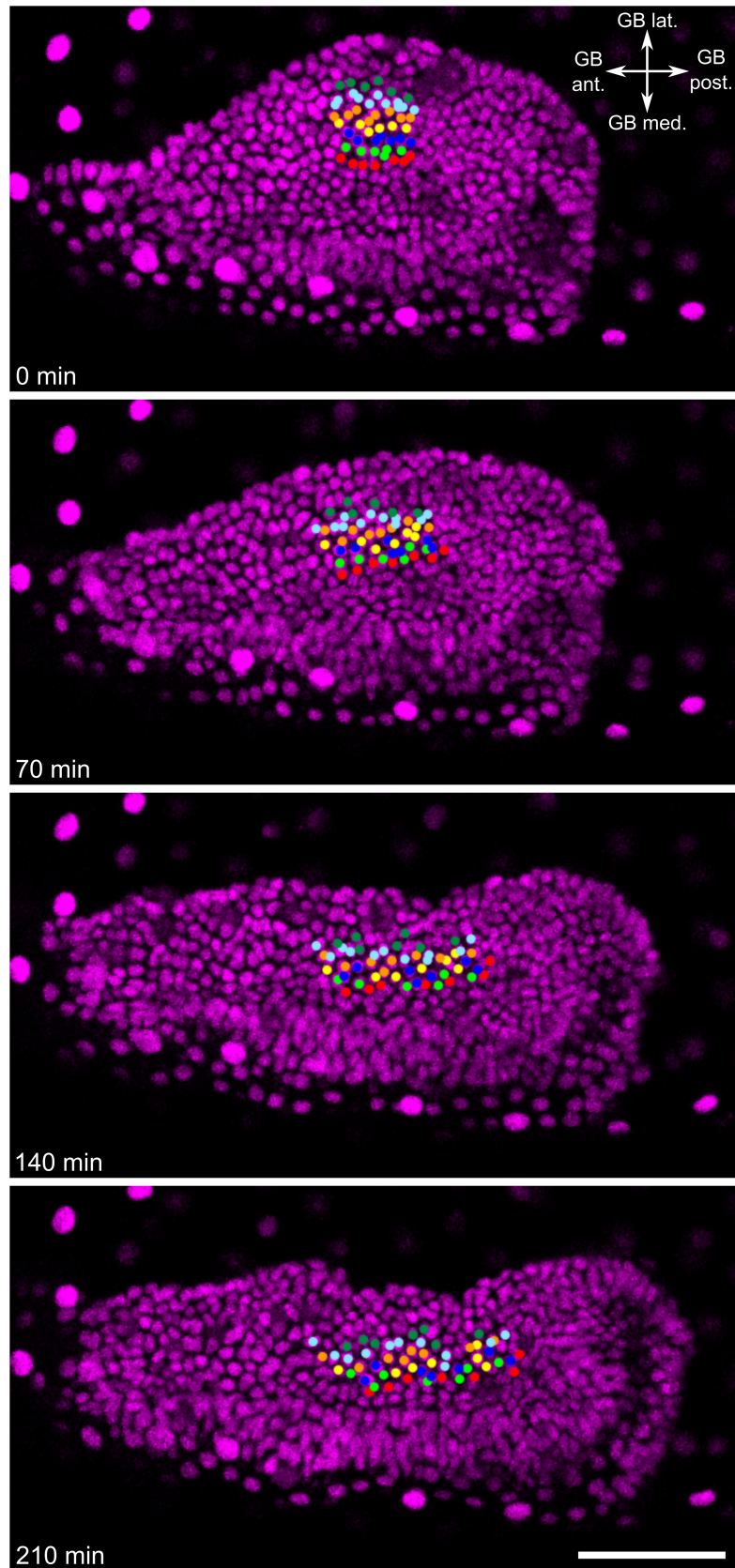


**Fig 4. Mediolateral cell intercalation occurs in the SAZ during GBE.** Time series from fluorescent live imaging of a *Tribolium* embryo expressing NLS-tdEos showing the SAZ during abdominal segment formation. Coloured points mark tracked nuclei. During the timelapse, nuclei underwent apicobasal movement, but I observed no cell delamination. Note that the same embryo is shown in Fig 3A–3F. The first frame of the timelapse was defined as time point 0. The embryo is oriented based on polarity of the visible region of the germband. Panels show maximum intensity projections of 15  $\mu\text{m}$  to specifically show the germband. The scale bar is 50  $\mu\text{m}$ . ant, anterior; GB, germband; GBE, germband extension; lat, lateral; med, medial; NLS-tdEos, nuclear localisation signal-tandem Eos; post, posterior; SAZ, segment addition zone.

<https://doi.org/10.1371/journal.pbio.2005093.g004>

embryo and presumptive serosa (summarised in Fig 6 and S6 Fig). At 50% EL, only approximately the 6 most dorsal cells (approximately 8% of the circumference of the blastoderm) gave rise to all amnion cells stretching from one side of the thorax to the other (Fig 5C, S1 Fig). Nearer to the posterior of the blastoderm (25% EL), even fewer cells gave rise to amnion (approximately 3 of the most dorsal cells; approximately 6% of the circumference; Fig 5D, S2 Fig). The posterior limit of the amnion was difficult to define, as although some cells from approximately 5%–10% EL appeared to become amnion (Fig 5E), these cells condensed posteriorly towards the hindgut during germband retraction and might have contributed to the hindgut tissue (S3 Fig, S7 Movie). I was unable to unambiguously determine the fate of these cells. At the anterior of the embryo, I found that a narrow strip of 1–2 cells between the presumptive embryo and presumptive serosa also gave rise to amnion (Fig 3G–3J). While substantial additional work will be required to define a complete blastoderm fate map for *Tribolium*, my findings clearly demonstrate that the ‘amnion’ domain is drastically smaller than previously proposed.

## Discussion

In this article, I have shown that a majority of the cells currently thought to be extraembryonic amnion actually give rise to embryonic tissue. Movement of these cells from the dorsal side of the germband to the ventral side was visible in live cell tracking and differential cell labelling experiments. My results also indicate that the true amnion region differentiates progressively along the AP axis during GBE, as evidenced by differences in cell behaviour and the expression of the gene *Tc-srp*. Lastly, presumptive amnion cells predominantly originate from a small domain on the dorsal side of the blastoderm.

## A revised understanding of the short germ embryo

The revision to the *Tribolium* blastoderm fate map that I describe is essentially a quantitative shift in our understanding of where cell fate boundaries lie along the DV axis. In the revised fate map (Fig 6, S6 Fig), the proportion of the blastoderm that gives rise to the presumptive amnion is much smaller than previously thought. The presumptive amnion domain is, therefore, remarkably similar in size to the amnioserosa domain of the *Drosophila* blastoderm fate map [18]. However, it is important to recognise that fate maps such as those presented here show a static picture of a dynamic process. There is no evidence that the presumptive amnion is specified at the blastoderm stage in *Tribolium*. Instead, the progressive changes in cell shape and activation of *Tc-srp* expression in the dorsal epithelium of the germband suggest that the amnion is specified progressively along the AP axis during GBE. Progressive specification of DV cell fates during GBE fits with previous hypotheses [36,46], and analysis of how this process occurs represents an exciting avenue of future research (a possible mechanism for DV patterning during GBE is discussed in S1 Text).

In contrast to the fate map revision, the observation that cells move from the dorsal half of the germband to the ventral half of the germband represents a qualitative shift in our

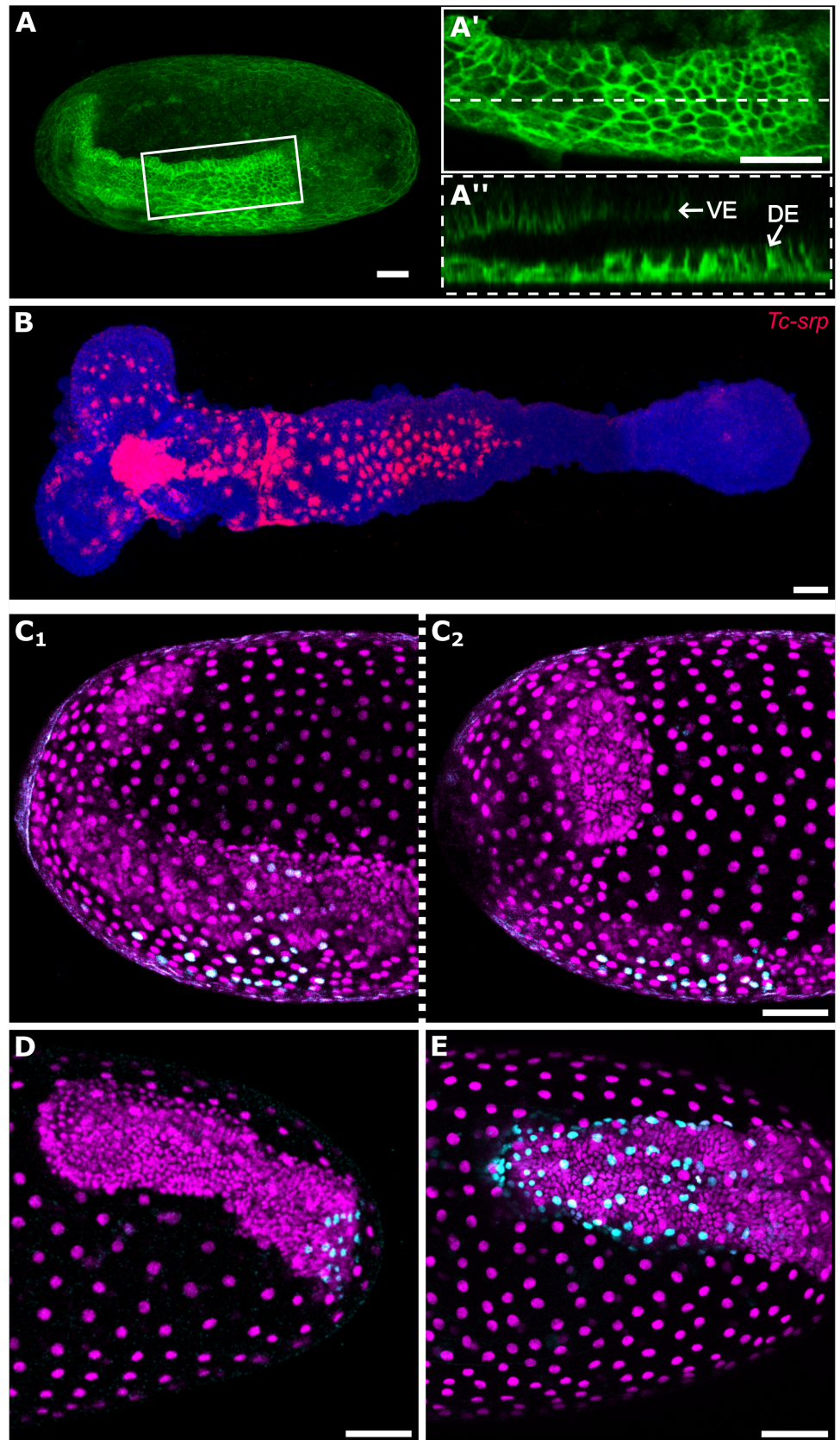


**Fig 5. Development of the putative amnion.** (A–A'') *Tribolium* embryo transiently expressing the membrane marker GAP43-YFP. (A) shows an overview of the whole egg, (A') shows the dorsal epithelium of the same embryo at the position of the white box, (A'') is an optical sagittal section at the position of the dashed line in (A') showing the apical-basal height of cells of the dorsal epithelium. (B) *Tc-srp* (red) expression in a flat-mounted *Tribolium* germband also showing nuclei (DAPI, blue). The strong *Tc-srp* signal in nuclei may suggest nuclear or perinuclear localisation of the transcript, or it may be due to the cell body being flattened. Aside from the strong patch of anterior medial expression (which is from cells beneath the embryonic ectoderm), all visible expression is in the putative amnion epithelium. (C–E) Extended germband stage *Tribolium* embryos transiently expressing NLS-tdEos showing unconverted protein (magenta) and photoconverted protein (cyan). In each embryo, the clone of converted cells spans the entire amnion. (C<sub>1–2</sub>) show both sides of the same embryo in which a 6-nuclei-wide patch of dorsalmost cells located at 50% EL was photoconverted at the blastoderm stage. (D) shows an embryo in which a 3-nuclei-wide patch of dorsalmost cells located at 25% EL was photoconverted at the blastoderm stage. (E) shows an embryo in which a 3-nuclei-wide by 6-nuclei-long patch of dorsalmost cells located at roughly 2%–10% EL were photoconverted at the blastoderm stage. In (A) and (C–E), embryos are oriented based on the AP/DV polarity of the egg with anterior to the left and dorsal to the top. In (A''), the surface of the egg is oriented to the bottom. In (B), the anterior of the germband is to the left. (A) is an average intensity projection of one egg hemisphere. (A') is an average intensity projection of 6 μm to specifically show the dorsal epithelium. (B) is a maximum intensity projection of the whole germband. (C–E) are maximum intensity projections of one egg hemisphere. Scale bars are 50 μm. AP, anterior-posterior; DE, dorsal ectoderm; DV, dorsoventral; EL, egg length; GAP43-YFP, GAP43-yellow fluorescent protein; NLS-tdEos, nuclear localisation signal-tandem Eos; *Tc-srp*, *Tribolium* ortholog of the GATA factor *serpent*; VE, ventral ectoderm.

<https://doi.org/10.1371/journal.pbio.2005093.g005>

understanding of development in short/intermediate germ insects. In the classic model of short/intermediate germ development, the germband was thought of as a more or less flat sheet of ectodermal cells (with mesoderm underneath) covered by the extraembryonic amnion. Because of this, the entire dorsal epithelium is routinely removed during embryo preparation, or not included in descriptions of gene expression patterns and embryonic phenotypes. Based on the new data presented here, it is obvious that we have been discarding or ignoring large parts of the embryo. Furthermore, the movement of cells from the dorsal epithelium into the ventral epithelium must be contributing to GBE and is, therefore, a key aspect of the extension and overall development of the germband that has thus far been missed.

The revised model of the germband does present some technical challenges for future work on short/intermediate germ embryo. The flattened geometry of the germband makes it difficult to image both the dorsal and ventral epithelium using bright-field microscopy approaches. However, this problem can be overcome either by using fluorescence based techniques and confocal microscopy or by mechanical sectioning of the germband. Both approaches have been shown to work well in *Tribolium* (for examples, see [13,47] and the results in this manuscript). In the rest of this article, I discuss why the revised fate map and cell flow accord well with what we know about *Tribolium* development and outline the implications of this discovery on our understanding of the evolution of insect development.

## The cellular and molecular causes of tissue flow unify the blastoderm and the germband

The revised model of the *Tribolium* germband reconciles the blastoderm and germband stages. The ectoderm of the germband is a continuous epithelium, which means that the movement of cells from the dorsal epithelium to the ventral epithelium occurs as a tissue level 'flow'. Such dorsal-to-ventral tissue flow also occurs during embryo condensation in *Tribolium* [14], and I propose that the flow is caused by largely the same morphogenetic processes at both stages. The evidence for this hypothesis is summarised here, but for an extended discussion see [S2 Text](#).

Three morphogenetic processes contribute to dorsal-to-ventral cell flow in *Tribolium*, and at least two of the three occur at both the blastoderm and germband stages. First, mediolateral cell intercalation occurs at both stages and causes tissue-wide convergence (along the DV axis)

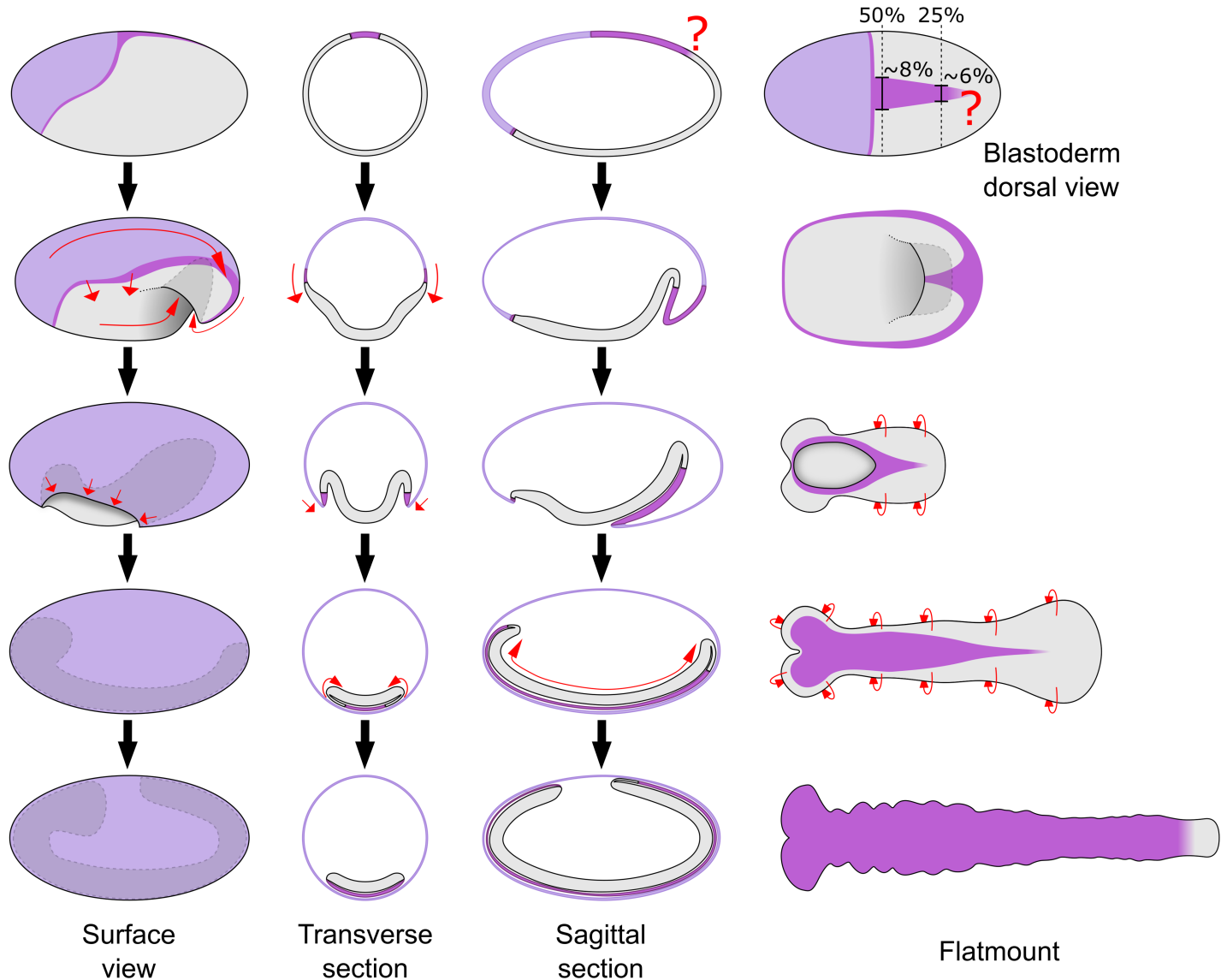


**Fig 6. Schematics showing the revised *Tribolium* amnion fate map and germband model.** Schematics drawn as in Fig 1 to show the revised fate map (top row; drawn directly from the numbers described in the text) and germband model based on the results of this manuscript. Note that the posterior amnion/embryo boundary is unclear. The schematics of the flat-mounted germbands are drawn with the focus on the dorsal epithelium. See text for additional details, and S6 Fig for an extended figure with the classic and revised models side-by-side.

<https://doi.org/10.1371/journal.pbio.2005093.g006>

and extension (along the AP axis). This process requires two *Toll* genes that are expressed in rings around the entire blastoderm and germband epithelium [17]. Second, tissue-specific cell shape changes occur at both stages such that ventral/lateral cells become columnar and dorsal/dorsolateral cells become thinner (during condensation [S7 Fig]) or squamous (during GBE). The tissue level effect of these changes is contraction of the ventral/lateral ectoderm and spreading of the dorsal tissue. The flattening of dorsal/dorsolateral cells is likely regulated by Bone Morphogenetic Protein (BMP) signalling, as not only does BMP activity correlate with the cell shape changes (see S2 Text), but functional disruption of BMP signalling components leads to uniform cell shape changes along the DV axis [25,48]. A third major morphogenetic event is gastrulation of the mesoderm. This occurs along the ventral midline, and as

gastrulation occurs, the ectoderm moves ventrally to seal the gap left in the epithelium [47]. At the stage when a complete germband has formed, gastrulation is complete along most of the embryo. However, current data suggest mesoderm gastrulation may be ongoing in the SAZ [47]. If true, the ongoing invagination would contribute to tissue flow in this region.

It is important to note that while each of the events described here is involved in the dorsal-to-ventral tissue flow, no single event is absolutely required for it. In the absence of cell intercalation, embryo condensation and thinning of dorsal/dorsolateral ectoderm still takes place, yielding abnormally wide and short germbands [17]. In the absence of tissue-specific cell shape changes, condensation occurs in a more radially symmetrical manner, yielding a tube-shaped germband that undergoes segment specification and convergent extension [25,48]. Finally, both condensation and GBE are only mildly affected in the absence of mesoderm specification [49]. This functional independence comes from each of the three processes being specified by different pathways (intercalation via segment specification, dorsal thinning via dorsal tissue specification, and gastrulation via ventral tissue specification). There may also be further, as yet undiscovered, morphogenetic events that also contribute to the dorsal-to-ventral tissue flow.

## Reconciling long and short germ development

I propose that the dorsal-to-ventral tissue flow occurring during embryo condensation and GBE in *Tribolium* is homologous to the dorsal-to-ventral tissue flow that occurs during gastrulation and GBE in *Drosophila* (Fig 1). This conclusion is based on the flow being driven by a conserved set of morphogenetic events.

As described above, tissue flow in *Tribolium* is caused by (1) mediolateral cell intercalation, (2) tissue-specific cell shape changes along the DV axis, and (3) gastrulation at the ventral side of the embryo. As described below, equivalent processes are all observed in *Drosophila* as well.

In *Drosophila*, Toll-mediated mediolateral cell intercalation causes tissue-wide convergence (along the DV axis) and extension (along the AP axis) of the ectoderm during GBE [16]. As in *Tribolium*, the periodic expression of the Toll genes is regulated by the pair-rule genes. Conservation at the level of tissue identity, morphogenetic process, and molecular control strongly suggest Toll-mediated cell intercalation to be homologous.

Cell shape changes are harder to compare between *Drosophila* and *Tribolium*, because unlike in most insects, cellularisation in *Drosophila* leads to the direct formation of columnar cells [18,50]. However, tissue-specific cell shape changes along the DV axis do occur in *Drosophila* and are dependent on BMP signalling ([51,52]; for a detailed description see S3 Text). While the intracellular effectors of these cell shape changes are unknown, use of BMP signalling for dorsal patterning is homologous in *Drosophila* and *Tribolium*, and many dorsal cell specification genes are conserved between these two species [48].

Last, *Drosophila* mesoderm gastrulation also occurs along the ventral midline and causes lateral/dorsolateral ectoderm to move ventrally [51]. Similar to the tissue-specific cell shape changes described above, the intracellular effectors of *Tribolium* mesoderm gastrulation are unknown, but the upstream patterning events and the tissue specification genes are highly conserved [36,49]. Furthermore, mesoderm gastrulation at the ventral region of the embryo is widely observed within the insects and is undoubtedly a homologous process in each species [53].

While I have focused on *Tribolium* and *Drosophila* here, evidence exists that the new findings in *Tribolium* may also apply to other short/intermediate germ insects. For example, in the intermediate germ bug *Oncopeltus fasciatus* (which forms a condensed, multilayered germband with tissue topology similar to that of *Tribolium* [26]), the dorsal epithelium of the

germband initially consists of a thick epithelium, which progressively becomes squamous late during GBE [54]. These tissue-specific cell shape changes are likely the same as those occurring during *Tribolium* GBE. Furthermore, *Oncopeltus* pair-rule genes, *Loto Toll* genes, and even segment polarity genes are expressed in rings around the entire germband prior to thinning of the dorsal epithelium [17,55,56]. The expression of these genes in the dorsal epithelium provides additional evidence that much of the *Oncopeltus* dorsal epithelium is made up of embryonic tissue. Future analyses of the molecular and morphogenetic drivers of GBE must analyse the entire germband, rather than focusing on the ventral half. In addition, further work will be needed to determine whether the new findings in *Tribolium* also apply to more basally branching insects, such as crickets.

## Materials and methods

*Tribolium* animal husbandry, egg collection, and RNA in situ hybridisation was performed as previously described [17]. The *Tc-srp* ortholog was previously described [57] and was cloned into pGEM-t (Promega Reference A1360) with primers TCCCGCTGCTTTGATCTAGT and TGCGATGACTGTGACGTGTA. The *Tc-cad* ortholog was as previously used [14].

The *H2B-ven* fusion was created by fusing the *D. melanogaster* histone *H2B* coding sequence (without the stop codon) from the published H2B-RFP [14] to the *venus* fluorescent protein [58] and cloning into the pSP64 Poly(A) (Promega Reference P1241) expression vector. The *NLS-tdEos* fusion was kindly provided by Matthias Pechmann. Additional details and both plasmids are available upon request to M. Pechmann or myself. Capped mRNA synthesis was performed as previously described [14]. *H2B-ven* capped mRNA was injected at 1  $\mu\text{g}/\mu\text{L}$ ; *NLS-tdEos* capped mRNA was injected at 2–3  $\mu\text{g}/\mu\text{L}$ .

Embryo microinjection was performed as previously described [14], with the following changes. Up to 100 dechorionated embryos were mounted on a rectangular coverslip (24 mm by 50 mm) that rested on a microscope slide. Water was allowed to dry off the embryos before they were covered in Voltaef 10S halocarbon oil and injected as usual. The coverslip (still resting on the slide) was then placed in a petri dish (92 mm) containing a base layer of 1% agarose (dissolved in water) and placed at 30–32°C until the embryos were at the appropriate stage for imaging. The coverslip was then removed from the slide, inverted (so that embryos were face down), and quickly but gently placed on a lumox dish (50 mm; Sarstedt Reference 94.6077.410) that was sitting upside down. The corners of the coverslip rested on the raised plastic lip of the dish such that the membrane and embryos were close to each other but not touching. To ensure lateral stability of the coverslip during the timelapse recording, approximately 5–10  $\mu\text{L}$  of heptane glue (made by soaking parcel tape in heptane) was placed at each corner. Additional Voltaef 10S halocarbon oil was then added to fill any remaining space between the coverslip and the oxygen permeable membrane. This contraption was then stuck to a microscope slide (using double sided tape) for imaging on an upright microscope. This last step may be unnecessary depending on the microscope stage and orientation.

Live imaging was performed on an upright Zeiss SP8 confocal microscope equipped with Hybrid detectors in the Biocentre Imaging facility (University of Cologne). Image stacks of 15–50 focal planes with z-steps ranging from 2–10  $\mu\text{m}$  were taken with a 10 $\times$ /0.3NA dry objective or a 20 $\times$ /0.7NA multi-immersion objective at intervals of 5–45 minutes. The temperature of the sample during imaging could not be carefully regulated but was typically between 25 and 28 degrees. While this lack of temperature control is not ideal, it does not affect the findings presented in this manuscript.

Photoconversion of NLS-tdEos protein was performed by constantly scanning the region of interest for 20–30 seconds with the 405 wavelength laser at low power (5%). These settings

were manually determined on the above microscope, and need to be determined independently on different systems. Photoconversions were performed during the final uniform blastoderm stage, as photoconversion prior to this resulted in substantial diffusion of the photoconverted protein during nuclei division. The positions of the different regions of the embryo (75% EL, etc.) were determined by measuring the length of each embryo in the LASX software and selecting the appropriate region. Photoconversions were performed on all embryos on the coverslip before setting up the timelapse, which led to a 0.5–2 hour delay between performing the photoconversion and beginning the timelapse. As such, the positions of the photoconverted region at the first time point in the timelapses in this manuscript do not reflect the original region of photoconversion.

Imaging of fixed material was performed on an upright Zeiss SP8 confocal, an upright Zeiss SP5 confocal microscope, and an inverted Zeiss SP5 confocal microscope. Images and timelapses were analysed using FIJI [59] and Photoshop CS5. Manual cell tracking was performed on confocal hyperstacks with MTrackJ [60]. The figures were arranged and the schematics created using Inkscape.

## Supporting information

**S1 Fig. Results of photoconversions at 50% egg length.** NLS-tdEos-labelled extended germ-band stage *Tribolium* embryos in which a patch of blastoderm nuclei was photoconverted at 50% egg length (from the posterior pole) at different DV positions. The approximate DV position of the patch and the approximate DV width of the clone (in terms of nuclei number) are shown. The dorsal labelled embryo is shown from both sides to demonstrate the photoconverted nuclei cover the full DV extent of the amnion (arrows). Unconverted protein is shown in magenta; converted protein is shown in cyan. Images are maximum intensity projections of one egg hemisphere. All eggs are oriented with the anterior to the left and ventral to the bottom. Scale bars are 100  $\mu\text{m}$ . DV, dorsoventral; NLS-tdEos, nuclear localisation signal-tandem Eos.

(TIF)

**S2 Fig. Results of photoconversions at 25% egg length.** NLS-tdEos-labelled extended germ-band stage *Tribolium* embryos in which a patch of blastoderm nuclei were photoconverted at 25% egg length (from the posterior pole) at different DV positions. The approximate DV position of the patch and the approximate DV width of the clone (in terms of nuclei number) are shown. Unconverted protein is shown in magenta; converted protein is shown in cyan. Images are maximum intensity projections of one egg hemisphere. All eggs are oriented with the anterior to the left and ventral to the bottom. Scale bars are 100  $\mu\text{m}$ . DV, dorsoventral; NLS-tdEos, nuclear localisation signal-tandem Eos.

(TIF)

**S3 Fig. Results of photoconversions near the posterior pole.** NLS-tdEos-labelled extended germ-band stage *Tribolium* embryos in which a patch of blastoderm nuclei were photoconverted near the posterior pole at different DV positions. The approximate DV position of the patch and the approximate DV width of the clone (in terms of nuclei number) are shown. The second dorsally labelled embryo is shown at high magnification at two time points and with a transverse section (at the position of the dashed green line) to show the movement of tissue from the dorsal epithelium into the hindgut. Unconverted protein is shown in magenta; converted protein is shown in cyan. Images are maximum intensity projections of one egg hemisphere except for the bottom three embryos, which are shown as maximum intensity projects through the germband in order to better show the labelled nuclei. All eggs are oriented with

the anterior to the left and ventral to the bottom except for the second time point of the second dorsal view, which is shown with the posterior of the germband to the left. Scale bars are 100  $\mu\text{m}$ . DV, dorsoventral; NLS-tdEos, nuclear localisation signal-tandem Eos.

(TIF)

**S4 Fig. RNA expression of the *Tribolium* ortholog of the GATA factor *serpent*.** (A-F) whole mount and (G-J) flat-mount *Tribolium* embryos from the pre-blastoderm to the retracting germband stage stained for *Tc-srp* mRNA (red) and nuclei (DAPI, blue). ( $G_1$ ) and ( $G_2$ ) show the same embryo imaged from both sides. ( $H_1$ ) and ( $H_2$ ) show projections from the dorsal epithelium ( $H_1$ ) and the ventral epithelium ( $H_2$ ) of the same embryo. *Tc-srp* mRNA is maternally provided (A), and expression is ubiquitous until the late blastoderm stage (B-C), when expression clears from the blastoderm but persists in the yolk nuclei (scattered spots in [D-E]). During embryo condensation, de novo expression arises in a patch of blastoderm cells at the anterior medial region (arrowhead in F). This patch of *Tc-srp*-expressing cells invaginates as part of the ventral furrow and becomes located beneath the ectoderm (arrowhead in  $G_1$ - $H_3$ ). This expression domain is likely homologous to the anterior ventral expression domain in *Drosophila* that marks the prohemocytes. During serosa window closure, expression appears in a ring of dorsal epithelium cells ( $G_1$ ). After serosa window closure, expression persists in the dorsal epithelium ( $H_1$ ) and ( $H_3$ ). Unlike *Drosophila*, there is no expression domain at the posterior of the blastoderm (E) or the early germband ( $G_2$ ). After germband elongation, a de novo expression domain appears at the posteriormost point of the embryo ( $I_1$ ). Given the location of this domain at the base of the forming hindgut, this is likely the posterior endoderm primordium. Expression can also be seen in a patch of amnion that has remained attached to the germband (arrow in  $I_2$ ), but most of the rest of the amnion has been lost. Several other regions of expression can be seen, including in the presumptive fat body (the segmental domains running down the body), in presumptive hemocyte clusters (the two side-by-side domains in the anterior), and in an anterior domain that may mark the anterior endoderm primordium. Expression also persists in the yolk nuclei (visible in the remaining yolk fragments at the anterior of the germband in  $I_1$ ). All embryos are shown with anterior to the left. (E-E'') is oriented with the ventral to the bottom; (F-F'') is oriented as a ventral view. ( $H_3$ - $H_3''$ ) is an optical sagittal section at approximately the midline of the embryo in ( $H_2$ ). (A-F) are maximum intensity projections of one egg hemisphere. ( $G_1$ - $G_2''$ ), ( $I_1$ - $I_1''$ ), and ( $J$ - $J''$ ) are maximum intensity projections of flat-mounted germbands. ( $I_2$ - $I_2''$ ) is a maximum intensity projection of part of the germband to better show the amnion/dorsal epithelium. Scale bars are 50  $\mu\text{m}$ . *Tc-srp*, *Tribolium* ortholog of the GATA factor *serpent*.

(TIF)

**S5 Fig. Schematics showing the photoconversion approach to determine the amnion fate map.** A patch of nuclei (of known dimensions) was photoconverted at the blastoderm stage, then the same embryos were examined at the end of germband extension. In embryos in which all photoconverted nuclei were located in the amnion and these nuclei spanned the entire DV width of the amnion (as shown here), the number of nuclei initially photoconverted was used to determine the DV width of the blastoderm domain giving rise to the amnion. Note that the precise number and distribution of nuclei shown here were arbitrarily chosen. Blue shows photoconverted nuclei; yellow shows the yolk. The serosa is omitted from the bottom panels. DV, dorsoventral.

(TIF)

**S6 Fig. Extended schematics showing the classic and revised *Tribolium* amnion fate maps and germband models.** Schematics drawn as in Fig 1 to show the classic and revised fate maps

and germband models based on the results of this manuscript. The schematics of the flat-mounted germbands are drawn with the focus on the dorsal epithelium. See text for additional details.

(TIF)

**S7 Fig. Tissue-specific cell shape changes during *Tribolium* condensation.** Stills from time-lapses of two *Tribolium* embryos transiently expressing GAP43YFP to label membranes. The second panel of each time point shows optical transverse sections at the position of the dashed line in the related panel. Ventral and lateral ectoderm becomes columnar, while dorsal ectoderm becomes flattened. The non-columnar cells at the bottom of the left hand embryo are likely the presumptive mesoderm. The first frame of the timelapses was defined as time point 0. Both embryos are oriented with the anterior to the left and ventral to the bottom. Scale bars are 100  $\mu\text{m}$ . Dor, Dorsal; Ect, Ectoderm; GAP43YFP, GAP43-yellow fluorescent protein Lat, Lateral; Ven, Ventral.

(TIF)

**S1 Movie. Confocal timelapse of a *Tribolium* embryo transiently expressing H2B-ven to mark nuclei.** A maximum intensity projection of one egg hemisphere is shown. Anterior is to the left; the ventral side of the egg is to the bottom. H2B-ven, H2B-venus.

(MOV)

**S2 Movie. Same timelapse as S1 Movie, but with nuclei of the dorsal epithelium tracked until they join the ventral epithelium.** Nuclei that join the ventral epithelium are labelled magenta, nuclei that become located at the edge of the germband are labelled yellow, and nuclei that remain in the dorsal epithelium are labelled cyan. Anterior is to the left; the ventral side of the egg is to the bottom. See [Fig 2A–2C](#) for more details.

(MOV)

**S3 Movie. Same timelapse as S1 Movie, but with a line of nuclei of the dorsal epithelium tracked.** Nuclei that remain in the dorsal epithelium are labelled cyan. Anterior is to the left; the ventral side of the egg is to the bottom. See [Fig 2D–2F](#) for more details.

(MOV)

**S4 Movie. Confocal timelapse of a *Tribolium* embryo transiently expressing NLS-tdEos (magenta) with a line of blastoderm cells photoconverted (cyan).** The brightness increases approximately halfway through the movie because of a manual increase in laser power at this point. A maximum intensity projection of one egg hemisphere is shown. Anterior is to the left; the ventral side of the egg is to the bottom. NLS-tdEos, nuclear localisation signal-tandem Eos.

(MOV)

**S5 Movie. Confocal timelapse of a *Tribolium* embryo transiently expressing NLS-tdEos (magenta) with a patch of blastoderm cells photoconverted (cyan).** (A) shows a maximum intensity projection of one egg hemisphere. (B) shows an optical transverse section. (C) shows an average intensity projection of 10 optical transverse sections. Anterior is to the left; the ventral side of the egg is to the bottom. See [Fig 3A–3F](#) for more details. NLS-tdEos, nuclear localisation signal-tandem Eos.

(MOV)

**S6 Movie. Confocal timelapse of a *Tribolium* embryo expressing NLS-tdEos showing the SAZ during abdominal segment formation.** Coloured points mark tracked nuclei. The embryo is oriented based on polarity of the visible region of the germband, with posterior to the right and lateral to the top. Panels show maximum intensity projections of 15  $\mu\text{m}$  to

specifically show the germband. See Fig 4 for more details. NLS-tdEos, nuclear localisation signal-tandem Eos; SAZ, segment addition zone.

(MOV)

**S7 Movie. Confocal timelapse of a *Tribolium* embryo transiently expressing NLS-tdEos (magenta) with a patch of blastoderm cells photoconverted (cyan).** Towards the end of the timelapse, the cyan nuclei in the dorsal epithelium appear to condense posteriorly to the hind-gut. A maximum intensity projection of one egg hemisphere is shown. Anterior is to the left; the ventral side of the egg is to the bottom. NLS-tdEos, nuclear localisation signal-tandem Eos.

(MOV)

**S1 Text. Extended discussion of topics from discussion section ‘A revised understanding of the short germ embryo’.**

(DOCX)

**S2 Text. Extended discussions of topics from discussion section ‘cellular and molecular causes of tissue flow’.**

(DOCX)

**S3 Text. Extended discussions of topics from discussion section ‘reconciling long and short germ development’.**

(DOCX)

## Acknowledgments

I am very grateful to S. Roth for his generous support, and for the extensive and stimulating discussions throughout this project. I am also thankful to E. Clark for in-depth discussions and extensive feedback on the manuscript. I thank M. Pechmann for providing the *NLS-tdEos* construct. In addition, I thank M. Akam, M. Pechmann, and S. Roth for comments on the manuscript, and B. Schmitt for comments on the schematics.

## Author Contributions

**Conceptualization:** Matthew A. Benton.

**Investigation:** Matthew A. Benton.

**Methodology:** Matthew A. Benton.

**Visualization:** Matthew A. Benton.

**Writing – original draft:** Matthew A. Benton.

**Writing – review & editing:** Matthew A. Benton.

## References

1. Grimaldi D, Engel M. Evolution of the Insects. Cambridge University Press; 2005.
2. Anderson DT. Embryology and Phylogeny in Annelids and Arthropod. Pergamon Press; 1973.
3. Jaeger J. The gap gene network. Cell Mol Life Sci. 2011; 68: 243–74. <https://doi.org/10.1007/s00018-010-0536-y> PMID: 20927566
4. Davis GK, Patel NH. SHORT, LONG, AND BEYOND: Molecular and Embryological Approaches to. Annu Rev Entomol. 2002; 669–99. <https://doi.org/10.1146/annurev.ento.47.091201.145251> PMID: 11729088
5. Peel AD, Chipman AD, Akam M. Arthropod segmentation: beyond the *Drosophila* paradigm. Nat Rev Genet. 2005; 6: 905–16. <https://doi.org/10.1038/nrg1724> PMID: 16341071

6. Irvine KD, Wieschaus E. Cell intercalation during *Drosophila* germband extension and its regulation by pair-rule segmentation genes. *Development*. 1994; 120: 827–41. Available: <http://www.ncbi.nlm.nih.gov/pubmed/7600960> PMID: 7600960
7. Bertet C, Sulak L, Lecuit T. Myosin-dependent junction remodelling controls planar cell intercalation and axis elongation. *Nature*. 2004; 429: 667–671. Available: <https://doi.org/10.1038/nature02590> PMID: 15190355
8. Collinet C, Rauzi M, Lenne P, Lecuit T. Local and tissue-scale forces drive oriented junction growth during tissue extension. *Nat Cell Biol*. 2015; 17: 1247–1258. <https://doi.org/10.1038/ncb3226> PMID: 26389664
9. Butler LC, Blanchard GB, Kabla AJ, Lawrence NJ, Welchman DP, Mahadevan L, et al. Cell shape changes indicate a role for extrinsic tensile forces in *Drosophila* germ-band extension. *Nat Cell Biol*. Nature Publishing Group; 2009; 11: 859–64. <https://doi.org/10.1038/ncb1894> PMID: 19503074
10. Firmino AAP, Fonseca FC de A, de Macedo LLP, Coelho RR, Antonino de Souza JD Jr, Togawa RC, et al. Transcriptome Analysis in Cotton Boll Weevil (*Anthonomus grandis*) and RNA Interference in Insect Pests. *PLoS ONE*. 2013; 8: e85079. <https://doi.org/10.1371/journal.pone.0085079> PMID: 24386449
11. da Silva SM, Vincent J-P. Oriented cell divisions in the extending germband of *Drosophila*. *Development*. 2007; 134: 3049 LP–3054. Available: <http://dev.biologists.org/content/134/17/3049.abstract>
12. Liu PZ, Kaufman TC. Short and long germ segmentation: unanswered questions in the evolution of a developmental mode. *Evol Dev*. 2005; 7: 629–46. <https://doi.org/10.1111/j.1525-142X.2005.05066.x> PMID: 16336416
13. Sarrazin AF, Peel AD, Averof M. A segmentation clock with two-segment periodicity in insects. *Science*. 2012; 336: 338–41. <https://doi.org/10.1126/science.1218256> PMID: 22403177
14. Benton MA, Akam M, Pavlopoulos A. Cell and tissue dynamics during *Tribolium* embryogenesis revealed by versatile fluorescence labeling approaches. *Development*. 2013; 140: 3210–3220. <https://doi.org/10.1242/dev.096271> PMID: 23861059
15. Nakamoto A, Hester SD, Constantinou SJ, Blaine WG, Tewksbury AB, Matei MT, et al. Changing cell behaviours during beetle embryogenesis correlates with slowing of segmentation. *Nat Commun*. Nature Publishing Group; 2015; 6: 6635. <https://doi.org/10.1038/ncomms7635> PMID: 25858515
16. Paré AC, Vichas A, Fincher CT, Mirman Z, Farrell DL, Mainieri A, et al. A positional Toll receptor code directs convergent extension in *Drosophila*. *Nature*. 2014; 515: 523–527. <https://doi.org/10.1038/nature13953> PMID: 25363762
17. Benton MA, Pechmann M, Frey N, Stappert D, Conrads KHKH, Chen Y-TY-T, et al. Toll Genes Have an Ancestral Role in Axis Elongation. *Curr Biol*. Elsevier Ltd; 2016; 26: 1609–1615. <https://doi.org/10.1016/j.cub.2016.04.055> PMID: 27212406
18. Campos-Ortega J a, Hartenstein V. The embryonic development of *Drosophila melanogaster*. 2nd ed. Springer-Verlag Berlin Heidelberg; 1997.
19. Schönauer A, Paese CLB, Hilbrant M, Leite DJ, Schwager EE, Feitosa NM, et al. The Wnt and Delta-Notch signalling pathways interact to direct pair-rule gene expression via caudal during segment addition in the spider *Parasteatoda tepidariorum*. *Development*. 2016; 2455–2463. <https://doi.org/10.1242/dev.131656> PMID: 27287802
20. Janssen R. Gene expression suggests double-segmental and single-segmental patterning mechanisms during posterior segment addition in the beetle *Tribolium castaneum*. *Int J Dev Biol*. 2014; 58. <https://doi.org/10.1387/ijdb.140058jr> PMID: 25354454
21. Clark E. Dynamic patterning by the *Drosophila* pair-rule network reconciles long-germ and short-germ segmentation. Desplan C, editor. *PLoS Biol*. 2017; 15: e2002439. <https://doi.org/10.1371/journal.pbio.2002439> PMID: 28953896
22. van der Zee M, Berns N, Roth S. Distinct Functions of the *Tribolium* *zerknüllt* Genes in Serosa Specification and Dorsal Closure. *Curr Biol*. 2005; 15: 624–636. <https://doi.org/10.1016/j.cub.2005.02.057> PMID: 15823534
23. Falciani F, Hausdorf B, Schröder R, Akam M, Tautz D, Denell R, et al. Class 3 Hox genes in insects and the origin of zen. *Proc Natl Acad Sci USA*. 1996; 93: 8479–8484. PMID: 8710895
24. Handel K, Grünfelder CG, Roth S, Sander K. *Tribolium* embryogenesis: a SEM study of cell shapes and movements from blastoderm to serosal closure. *Dev Genes*. 2000;
25. Nunes da Fonseca R, von Levetzow C, Kalscheuer P, Basal A, van der Zee M, Roth S. Self-Regulatory Circuits in Dorsoventral Axis Formation of the Short-Germ Beetle *Tribolium castaneum*. *Dev Cell*. 2008; 14: 605–615. <https://doi.org/10.1016/j.devcel.2008.02.011> PMID: 18410735

26. Schmidt-Ott U, Kwan CW. Morphogenetic functions of extraembryonic membranes in insects. *Curr Opin Insect Sci*. Elsevier Inc; 2016; 13: 86–92. <https://doi.org/10.1016/j.cois.2016.01.009> PMID: [27436557](https://pubmed.ncbi.nlm.nih.gov/27436557/)
27. Panfilio K a. Extraembryonic development in insects and the acrobatics of blastokinesis. *Dev Biol*. 2008; 313: 471–91. <https://doi.org/10.1016/j.ydbio.2007.11.004> PMID: [18082679](https://pubmed.ncbi.nlm.nih.gov/18082679/)
28. Benton MA, Pavlopoulos A. Tribolium embryo morphogenesis: May the force be with you. *Bioarchitecture*. 2014; 4: 16–21. <https://doi.org/10.4161/bioa.27815> PMID: [24451992](https://pubmed.ncbi.nlm.nih.gov/24451992/)
29. Schmidt-Ott U. The amnioserosa is an apomorphic character of cyclorrhaphan flies. *Dev Genes Evol*. 2000; 210: 373–376. <https://doi.org/10.1007/s004270050325> PMID: [11180843](https://pubmed.ncbi.nlm.nih.gov/11180843/)
30. Rafiqi AM, Lemke S, Ferguson S, Stauber M, Schmidt-Ott U. Evolutionary origin of the amnioserosa in cyclorrhaphan flies correlates with spatial and temporal expression changes of zen. *Proc Natl Acad Sci U S A*. 2008; 105: 234–9. <https://doi.org/10.1073/pnas.0709145105> PMID: [18172205](https://pubmed.ncbi.nlm.nih.gov/18172205/)
31. Rafiqi AM, Park C, Kwan CW, Lemke S, Schmidt-ott U. BMP-dependent serosa and amnion specification in the scuttle fly *Megaselia abdita*. 2012; 3382: 3373–3382. <https://doi.org/10.1242/dev.083873>
32. Kwan CW, Gavin-Smyth J, Ferguson EL, Schmidt-Ott U. Functional evolution of a morphogenetic gradient. Bronner M, editor. *Elife*. eLife Sciences Publications, Ltd; 2016; 5: e20894. <https://doi.org/10.7554/eLife.20894> PMID: [28005004](https://pubmed.ncbi.nlm.nih.gov/28005004/)
33. Caroti F, González Avalos E, González Avalos P, Kromm D, Noeske V, Wosch M, et al. In toto live imaging in scuttle fly *Megaselia abdita* reveals transitions towards a novel extraembryonic architecture. *bioRxiv*. 2018; Available: <http://biorxiv.org/content/early/2018/01/15/236364.abstract>
34. Jacobs CGC, Spaink HP, van der Zee M. The extraembryonic serosa is a frontier epithelium providing the insect egg with a full-range innate immune response. *Elife*. 2014; 3: 1–21. <https://doi.org/10.7554/eLife.04111> PMID: [25487990](https://pubmed.ncbi.nlm.nih.gov/25487990/)
35. Jacobs CGC, Van Der Zee M. Immune competence in insect eggs depends on the extraembryonic serosa. *Dev Comp Immunol*. 2013; 41. <https://doi.org/10.1016/j.dci.2013.05.017> PMID: [23732406](https://pubmed.ncbi.nlm.nih.gov/23732406/)
36. Lynch JA, Roth S. The evolution of dorsal-ventral patterning mechanisms in insects. *Genes Dev*. 2011; 25: 107–118. <https://doi.org/10.1101/gad.2010711> PMID: [21245164](https://pubmed.ncbi.nlm.nih.gov/21245164/)
37. Horn T, Panfilio KA. Novel functions for Dorsocross in epithelial morphogenesis in the beetle *Tribolium castaneum*. *Development*. 2016; 143: 3002–3011. <https://doi.org/10.1242/dev.133280> PMID: [27407103](https://pubmed.ncbi.nlm.nih.gov/27407103/)
38. Anderson DT. The Development of Holometabolous Insects. In: Counce SJ, Waddington CH, editors. *Developmental systems Insects*, Vol 1. New York: Academic Press; 1972. pp. 165–242.
39. Anderson DT. The Development of Hemimetabolous Insects. In: Counce SJ, Waddington CH, editors. *Developmental systems Insects*, Vol 1. New York: Academic Press; 1972. pp. 95–163.
40. Aranda M, Marques-Souza H, Bayer T, Tautz D. The role of the segmentation gene hairy in *Tribolium*. *Dev Genes Evol*. 2008; 218: 465–77. <https://doi.org/10.1007/s00427-008-0240-1> PMID: [18679713](https://pubmed.ncbi.nlm.nih.gov/18679713/)
41. Benton MA. Fluorescent live imaging of differentially labeled *Tribolium* embryos [Internet]. Database: figshare [Internet]. 2018. Available: [https://figshare.com/authors/Matthew\\_Benton/4693354](https://figshare.com/authors/Matthew_Benton/4693354)
42. Tomancak P, Berman BP, Beaton A, Weiszmann R, Kwan E, Hartenstein V, et al. Global analysis of patterns of gene expression during *Drosophila* embryogenesis. *Genome Biol*. England; 2007; 8: R145. <https://doi.org/10.1186/gb-2007-8-7-r145> PMID: [17645804](https://pubmed.ncbi.nlm.nih.gov/17645804/)
43. Hammonds AS, Bristow CA, Fisher WW, Weiszmann R, Wu S, Hartenstein V, et al. Spatial expression of transcription factors in *Drosophila* embryonic organ development. *Genome Biol*. England; 2013; 14: R140. <https://doi.org/10.1186/gb-2013-14-12-r140> PMID: [24359758](https://pubmed.ncbi.nlm.nih.gov/24359758/)
44. Tomancak P, Beaton A, Weiszmann R, Kwan E, Shu S, Lewis SE, et al. Systematic determination of patterns of gene expression during *Drosophila* embryogenesis. *Genome Biol*. England; 2002; 3: RESEARCH0088. <https://doi.org/10.1186/gb-2002-3-12-research0088> PMID: [12537577](https://pubmed.ncbi.nlm.nih.gov/12537577/)
45. Sam S, Leise W, Hoshizaki DK. The serpent gene is necessary for progression through the early stages of fat-body development. *Mech Dev*. 1996; 60: 197–205. Available: <http://www.ncbi.nlm.nih.gov/pubmed/9025072> PMID: [9025072](https://pubmed.ncbi.nlm.nih.gov/9025072/)
46. Sachs L, Chen YT, Drechsler A, Lynch JA, Panfilio KA, Lässig M, et al. Dynamic BMP signaling polarized by Toll patterns the dorsoventral axis in a hemimetabolous insect. *Elife*. 2015; 4. <https://doi.org/10.7554/eLife.05502> PMID: [25962855](https://pubmed.ncbi.nlm.nih.gov/25962855/)
47. Handel K, Basal A, Fan X, Roth S. *Tribolium castaneum* twist: gastrulation and mesoderm formation in a short-germ beetle. *Dev Genes Evol*. 2005; 215: 13–31. <https://doi.org/10.1007/s00427-004-0446-9> PMID: [15645317](https://pubmed.ncbi.nlm.nih.gov/15645317/)

48. van der Zee M, Stockhammer O, von Levetzow C, Nunes da Fonseca R, Roth S. Sog/Chordin is required for ventral-to-dorsal Dpp/BMP transport and head formation in a short germ insect. *Proc Natl Acad Sci U S A*. 2006; 103: 16307–12. <https://doi.org/10.1073/pnas.0605154103> PMID: 17050690
49. Stappert D, Frey N, von Levetzow C, Roth S. Genome-wide identification of *Tribolium* dorsoventral patterning genes. *Development*. 2016; 143: 2443–2454. <https://doi.org/10.1242/dev.130641> PMID: 27287803
50. van der Zee M, Benton MA, Vazquez-Faci T, Lamers GEM, Jacobs CGC, Rabouille C. Innexin7a forms junctions that stabilize the basal membrane during cellularization of the blastoderm in *Tribolium castaneum*. *Development*. 2015; 142: 2173–2183. <https://doi.org/10.1242/dev.097113> PMID: 26015545
51. Rauzi M, Krzic U, Saunders TE, Krajnc M, Zihel P, Hufnagel L, et al. Embryo-scale tissue mechanics during *Drosophila* gastrulation movements. *Nat Commun*. The Author(s); 2015; 6: 8677. Available: <https://doi.org/10.1038/ncomms9677> PMID: 26497898
52. Leptin M, Grunewald B. Cell shape changes during gastrulation in *Drosophila*. *Development*. 1990; 110: 73 LP–84. Available: <http://dev.biologists.org/content/110/1/73.abstract>
53. Roth S. Gastrulation in Other Insects. In: Stern CD, editor. *Gastrulation From Cells to Embryo*. New York: Cold Spring Harbor Laboratory Press; 2004. pp. 105–121.
54. Ewen-Campen B, Jones TEM, Extavour CG. Evidence against a germ plasm in the milkweed bug *Oncopeltus fasciatus*, a hemimetabolous insect. *Biol Open*. 2013; 2: 556–68. <https://doi.org/10.1242/bio.20134390> PMID: 23789106
55. Erezylmaz DF, Kelstrup HC, Riddiford LM. The nuclear receptor E75A has a novel pair-rule-like function in patterning the milkweed bug, *Oncopeltus fasciatus*. *Dev Biol*. Elsevier Inc.; 2009; 334: 300–10. <https://doi.org/10.1016/j.ydbio.2009.06.038> PMID: 19580803
56. Liu PZ, Kaufman TC. even-skipped is not a pair-rule gene but has segmental and gap-like functions in *Oncopeltus fasciatus*, an intermediate germband insect. *Development*. 2005; 132: 2081–92. <https://doi.org/10.1242/dev.01807> PMID: 15788450
57. Gillis WQ, Bowerman B a, Schneider SQ. The evolution of protostome GATA factors: molecular phylogenetics, synteny, and intron/exon structure reveal orthologous relationships. *BMC Evol Biol*. 2008; 8: 112. <https://doi.org/10.1186/1471-2148-8-112> PMID: 18412965
58. Nagai T, Ibata K, Park ES, Kubota M, Mikoshiba K, Miyawaki A. A variant of yellow fluorescent protein with fast and efficient maturation for cell-biological applications. *Nat Biotechnol*. Nature Publishing Group; 2002; 20: 87. Available: <https://doi.org/10.1038/nbt0102-87> PMID: 11753368
59. Schindelin J, Arganda-Carreras I, Frise E, Kaynig V, Longair M, Pietzsch T, et al. Fiji: an open-source platform for biological-image analysis. *Nat Methods*. 2012; 9: 676–82. <https://doi.org/10.1038/nmeth.2019> PMID: 22743772
60. Meijering E, Dzyubachyk O, Smal I. *Methods for cell and particle tracking*. [Internet]. 1st ed. *Methods in enzymology*. United States: Elsevier Inc.; 2012. <https://doi.org/10.1016/B978-0-12-391857-4.00009-4>